J. Fluid Mech. (1968), *vol.* 31, *part* 3, *pp.* 467–479
Printed in Great Britain

Effect of waves at a gas–liquid interface on a turbulent air flow

By LEONARD S. COHEN† AND THOMAS J. HANRATTY

Department of Chemistry and Chemical Engineering, University of Illinois, Urbana, Illinois

(Received 11 November 1966 and in revised form 25 September 1967)

Air flowing over a liquid surface encounters an increased resistance if waves are present. The relation of this increased resistance to the properties of the waves has been studied. Air and a liquid flowed co-currently in an enclosed channel which is 12 in. wide and 1 in. high and which is long enough so that flow in the air and the liquid and the interfacial structure are fully developed. The drag on interfaces with three-dimensional wave structures was found to increase with the square of the gas velocity and to depend more on the height of the waves than on other parameters characterizing the interface. The ratio of the equivalent sand roughness to the root-mean-square of the fluctuations in the height of the liquid film is approximately equal to $3\sqrt{2}$. The velocity profiles in the gas were found to be different from what has been reported for flows over sand roughened surfaces.

Introduction

If air blows over a liquid surface waves are generated and the drag of the air on the liquid is larger than if the interface remained smooth. It has been convenient to describe the effect of the structure of the interface by comparing drag measurements on liquid surfaces with those for roughened solid surfaces.

Turbulent velocity measurements in pipes and in channels with smooth and roughened solid surfaces can be correlated by the relation

$$u = \frac{2{\cdot}303u^*}{K}\log\left(\frac{y^+}{z}\right), \tag{1}$$

where u^* is the friction velocity, $y^+ = yu^*/\nu$ is the dimensionless distance from the interface, and K is von Kármán's constant $= 0{\cdot}4$. The parameter K is reported to be approximately the same for both smooth and rough solid surfaces and the parameter z depends on the roughness of the surface (Hinze 1961; Schlichting 1960). Velocity profiles over gas–liquid interfaces have been correlated by (1) and the interfaces have been characterized by the parameter z (Ursell 1956; Ellison, 1956).

One of the chief difficulties in interpreting measurements of the air flow over liquid surfaces is that most studies have not involved direct measurements of the

† Present address: United Aircraft, Hartford, Connecticut.

surface stress, the velocity profile, and the interfacial structure in the same experiment. Interest in two-phase flow problems encountered in engineering practice (Dukler 1963) has prompted a research programme in this laboratory involving the study of the interaction between a turbulent air stream and a flowing liquid film. This paper describes some of the results of this programme. It reports on the relation of the increased drag to the interfacial structure and of the effect of waves at an air–liquid interface on the velocity profile relation in the gas.

Measurements of the interfacial structure and of the stress for air–water flow have been presented by Lilleleht & Hanratty (1961 *a*, *b*). Studies of the concurrent flow of air and a liquid film in an enclosed channel have also been presented by Ellis & Gay (1959) and by van Rossum (1959). The present paper reports on a more comprehensive set of measurements than has been presented in previous publications. These measurements reveal effects of liquid waves on the turbulent velocity profile which were not noted previously, and they give a more definite relation between the interfacial stress and the wave structure.

In the earlier work of Lilleleht & Hanratty the effect of the resistance was discussed using a method based on equation (1) suggested by Hama (1954) and by Clauser (1956). The ratio of the air velocity to the friction velocity was plotted against the logarithm of the distance from the average level of the liquid. The downward displacement of this plot from that for flow over a smooth surface was used as a measure of the interfacial roughness. In order for this method to be valid it is necessary that the slope of the two plots be the same; i.e. that the von Kármán constant be the same for flow over wavy surfaces as for flow over smooth surfaces. A closer examination of the earlier measurements of Lilleleht & Hanratty and the more recent measurements of Cohen (1964) which are being presented in this paper has indicated that significant differences exist in the slopes of the logarithmic plots of the data. Therefore the method proposed by Clauser and by Hama has been abandoned and the effect of waves on the air resistance is discussed by comparing measured friction factors with those for smooth and roughened solid surfaces.

Description of the experiments

The system in which the experiments were conducted has been described in detail in previous papers (Hanratty & Engen 1957; Lilleleht & Hanratty 1961 *a*). A liquid film flows on the bottom of an enclosed horizontal Plexiglas channel and a turbulent air stream flows concurrently over the liquid film. The range of variables was extended over that used by Lilleleht & Hanratty (1961 *a*, *b*) by varying the viscosity of the liquid. Two liquids were used: water and a 40–50 weight per cent solution of glycerine in water (G–I). The flow conditions in the liquid are characterized by a Reynolds number, R, based on the height and the average velocity of the liquid film.

The aspect ratio of the channel (12 in. wide by 1·015 in. high) is large enough so that the flow in the centre may be considered as two-dimensional. The channel is long enough (21 ft.) so that fetch effects can be eliminated. The pressure gradient and the gas velocity profile in the fully developed region are measured with pressure taps on the top of the channel and with an impact tube. The Wahlen gauge used in previous work in this laboratory was replaced by a Flow Corporation micromanometer having a precision of $\pm 0{\cdot}0002$ in. of n-butanal.

If waves exist at the interface, the drag on the liquid will be greater than the stress at the top wall of the channel, and the velocity profile in the gas will be distorted. The effective shear stress at the gas–liquid interface can be calculated from the pressure drop and the distance of the maximum in the velocity profile from the interface by using a force balance (Hanratty & Engen 1957). The flow in the gas phase has been characterized by three Reynolds numbers. One of these, R_g, is based on the thickness of the gas layer and an average gas velocity defined over the whole gas space. Another, R_B, uses a length scale equal to twice the distance from the interface to the maximum in the velocity profile, $2a$, and a velocity scale, $\overline{u}_B$, equal to the average gas velocity defined over the region between the maximum and the interface. The Reynolds number, R_A, is defined for the top part of the gas space in the same manner as is R_B for the bottom part.

A light absorption technique similar to that developed by Lilleleht & Hanratty (1961 *a*) was used to measure the instantaneous height of the liquid film. A beam of light of about 0·4 mm diameter is transmitted through the channel and the flowing liquid film. The amount of light transmitted depends on the height of the film, and the sensitivity can be adjusted by putting a dye in the liquid. The light impinges on a RCA-6199 photomultiplier tube, and the electrical signal coming from the tube is a measure of the liquid height. A detailed description of the technique is presented in a thesis by one of the authors (Cohen 1964). Several changes were made on the original design by Lilleleht & Hanratty. By redesigning the optical system a much smaller beam of light could be focused on the air–liquid interface. It was found that the length of the lens system could be reduced and the intensity of the beam increased by inserting a Plexiglas rod in the light path. The 3 in. long by $\frac{3}{4}$ in. diameter rod used was fitted at one end with a brass cap containing a 0·4 mm hole. The 0·4 mm diameter parallel beam leaving the capped end of the rod was focused at the interface by using three Bausch and Lomb DCX-6-110 double convex lenses. A General Electric 1493 automotive bulb was used as the light source. Several filters were placed in the light bulb housing to provide a beam of approximately 530 mμ wave length. The chopped light beam and the a.c. amplifier used in previous work was replaced by a continuous light beam and a Minneapolis Honeywell Accu Data III model DISA-1003 wide-band amplifier.

Background light was minimized by enclosing the photomultiplier tube and light beam assemblies and portions of the channel near the measuring station. The signal from the photomultiplier tube consisted of d.c. and a.c. components. The d.c. component was measured with a Hewlett Packard 425 micro voltammeter. In order to analyse the a.c. component the signal was sent through a Thodarson-Meissner GEO-5 geophysical transformer, which had a measured flat frequency response down to 0·2 c/s. It furnished a 20 KΩ load resistance for the photomultiplier tube and a 1 KΩ secondary impedance to the amplifier in order to ensure a linear operation with low noise. A 1000 Ω resistor was placed in parallel with the transformer secondary to reduce any effect of the amplifier input impedance on the transfer circuit. Frequency spectra were measured using a Krohn-Hite Model 330-A ultra-low frequency band-pass filter and a Flow Corporation Model 12A1 random signal voltmeter. In previous work the wave height distribution was measured by examining visually a Visicorder record. This type of analysis is now accomplished with a Beckman Universal Eput and Timer Model 7360. This counter was modified by replacing the two original trigger level potentiometers with 10 K numerical read-out potentiometers. For a particular setting of the potentiometers, V_0, two quantities were measured: (i) the fraction of a specified time interval that the signal was above V_0, and (ii) the number of times in a specified time interval that the signal passed through the level V_0.

High-speed movies were taken of the wavy interface using a Cini-Kodak special camera with Kodak Tri-X negative movie film. Data from these films was obtained using a Vanguard Model M-16D motion analyser.

Characterization of the interface

The types of wave structures that are seen at the air–liquid interface have been described by Hanratty & Engen (1957). At low enough air rates no waves are visible at the interface. The first waves to appear at the interface with increasing

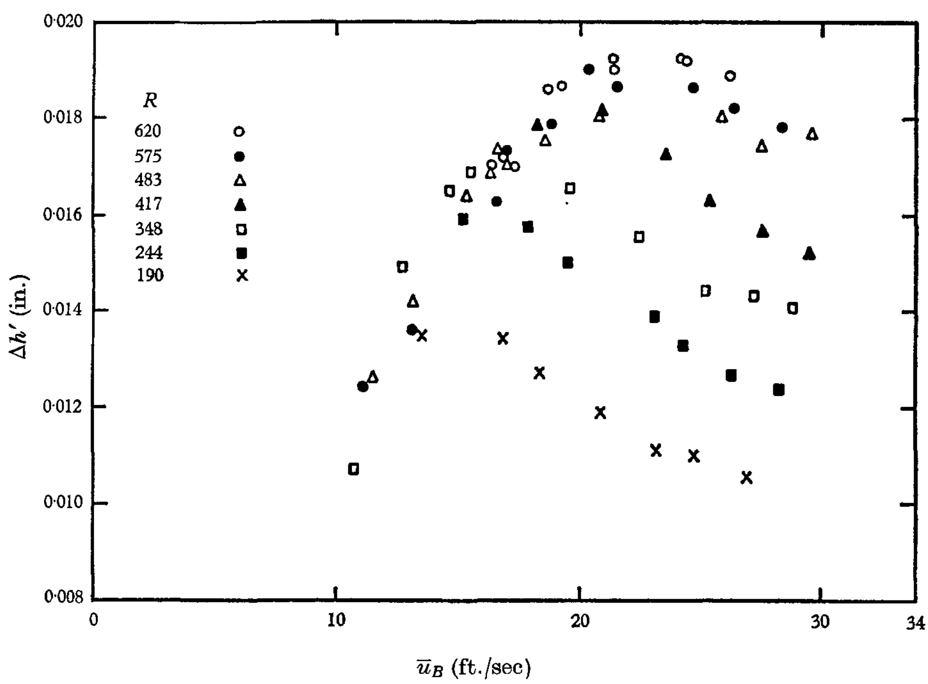

FIGURE 1. Root-mean-square wave heights, H_2O. $H_2O - \mu_L = 0{\cdot}98$ cP.

gas flow rate are two-dimensional waves. With further increase in the gas flow rate a three-dimensional pebbled wave structure appears. For the experiments described in this paper the wave pattern at the interface consisted of two-dimensional or three-dimensional waves.

The structure of the liquid interface may be characterized by root-mean-square wave heights, by frequency spectra, by wave height spectra, and by geometrical parameters taken from photographs. These techniques have been discussed in the paper by Lilleleht & Hanratty (1961*a*).

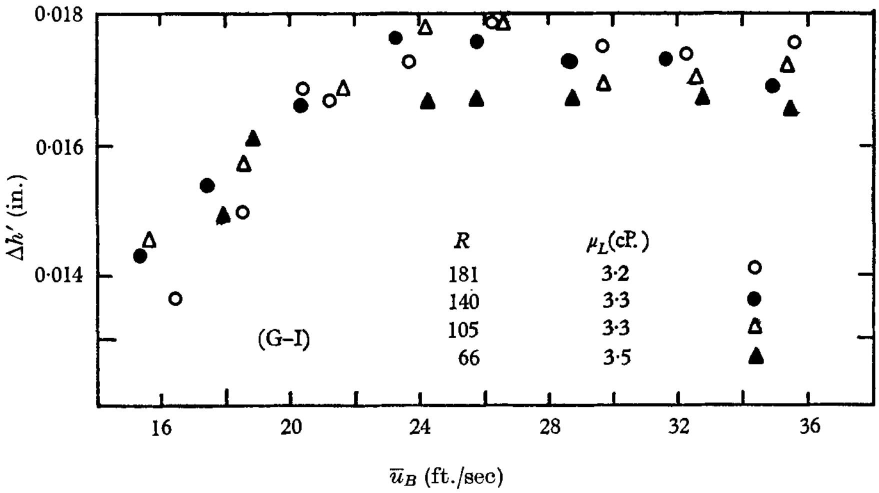

FIGURE 2. Root-mean-square wave heights, glycerine solutions.

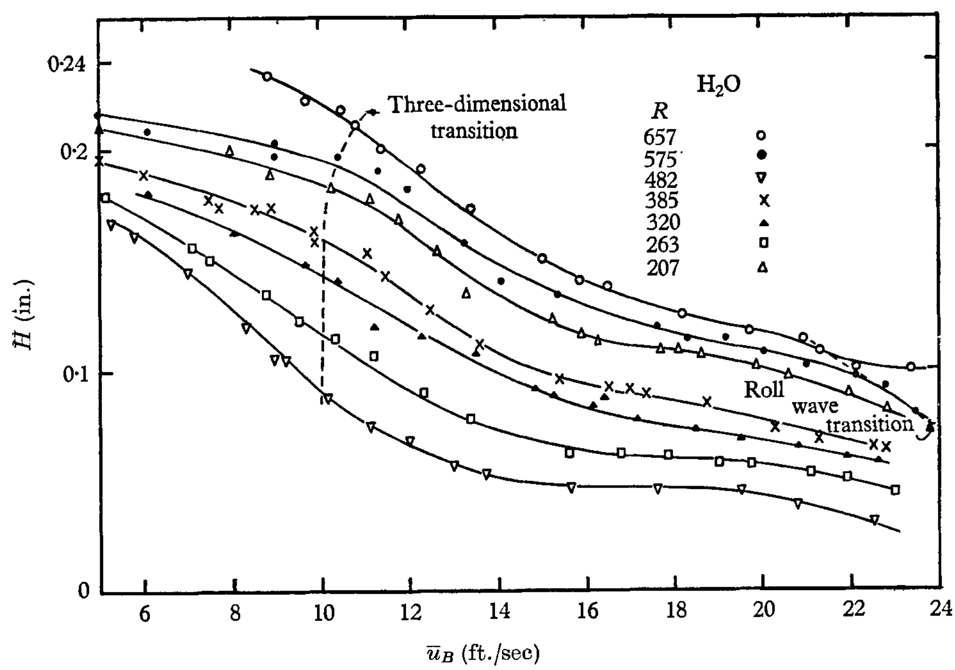

FIGURE 3. Measurements of the average film height for water.

Measurements of the root-mean-square wave heights $\Delta h'$ are presented in figures 1 and 2. Measurements of the average film height are presented in figures 3 and 4.

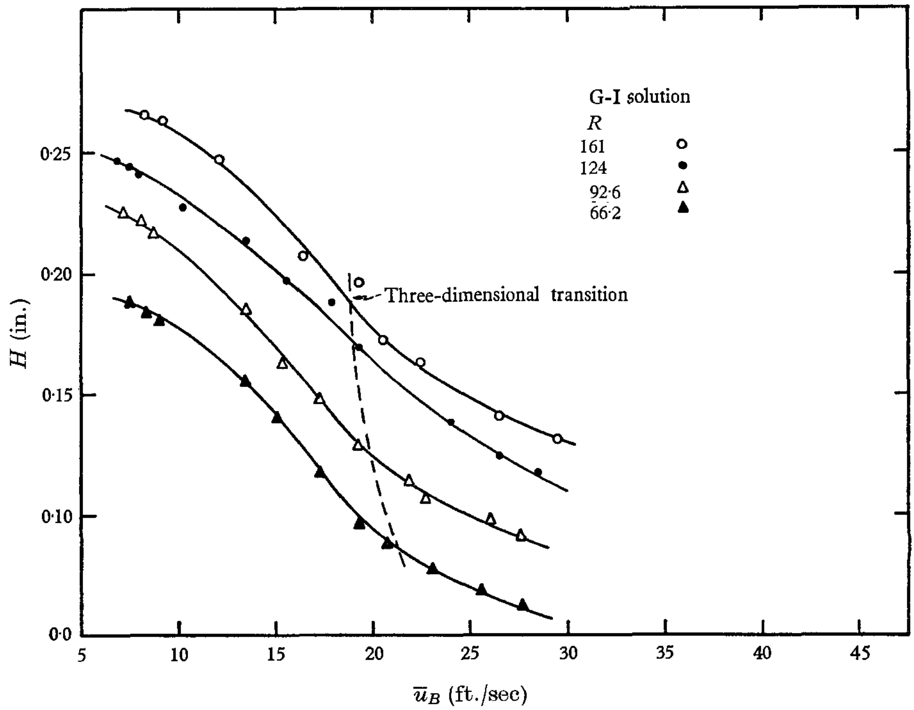

FIGURE 4. Measurements of the average film height for G–I solution.

The measured frequency spectra and amplitude distribution functions are presented in detail in the thesis of Cohen (1964). These measurements are more accurate and cover a wider range of variables than those reported by Lilleleht & Hanratty (1961*a*) on the same flow system. However, the results are quite similar and it is necessary here only to give a brief account of them. The spectra for all the systems showed a single maximum in the region of 7–12 c/s. Over the range of variables covered in this study ($H \geqslant 2$ mm) the amplitude distribution function describing the wave height is approximated quite accurately by a Gaussian distribution. The frequency spectra are consistent with this result in that the measured number of times the height is at the mean value agrees with that calculated from the frequency spectra using a Gaussian approximation. The number of crossings per second is in the range of 40–50.

Photographs of the interface when three-dimensional waves were present showed a cellular structure. The geometry of these cells was determined by measuring their average lengths in the Z- and X-directions The ratio of these lengths L_Z/L_X was found to be approximately equal to unity for the whole range of variables covered in this study. The length L_X decreased with increasing gas flow-rate. It varied from 0·25 to 0·5 in. for water and from 0·35 to 0·70 in. for the G–I solution.

Gas velocity profiles

A typical experimental gas velocity profile over a wavy liquid surface is shown in figure 5. The displacement of the maximum from the centre of the gas-space is a consequence of the different shear stresses at the boundaries. The shear stress at the interface τ_0 can be related to the profile displacement and the pressure drop in the channel if the shear stress at the maximum is taken to be zero:

$$-\frac{dP}{dx} = \frac{\tau_0}{a}. \tag{2}$$

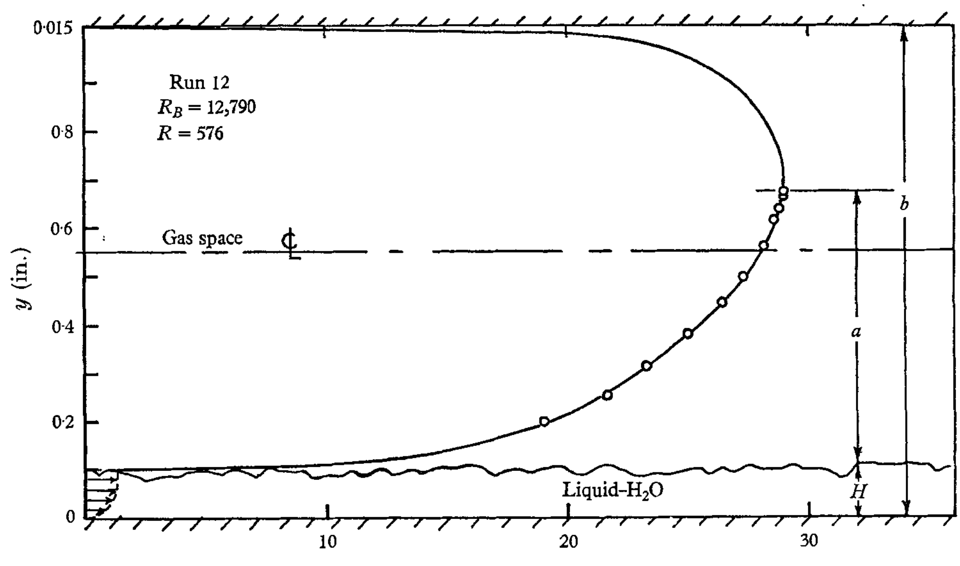

FIGURE 5. Experimental velocity profile.

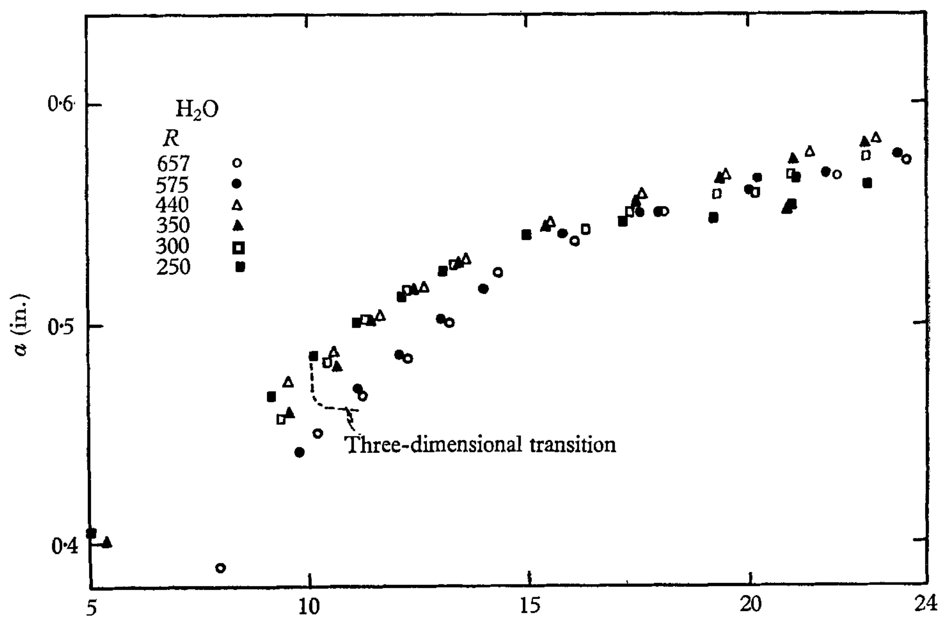

FIGURE 6. Distance from the maximum in the gas velocity profile to the interface.

Measured values of a are shown in figures 6 and 7. Justification for assuming the shear stress to be zero at the maximum in the velocity profile is obtained from the measurements of Brighton (1963) and from the good agreement between the correlation of velocity measurements in the top half of the channel and the correlation of velocity measurements in the dry channel.

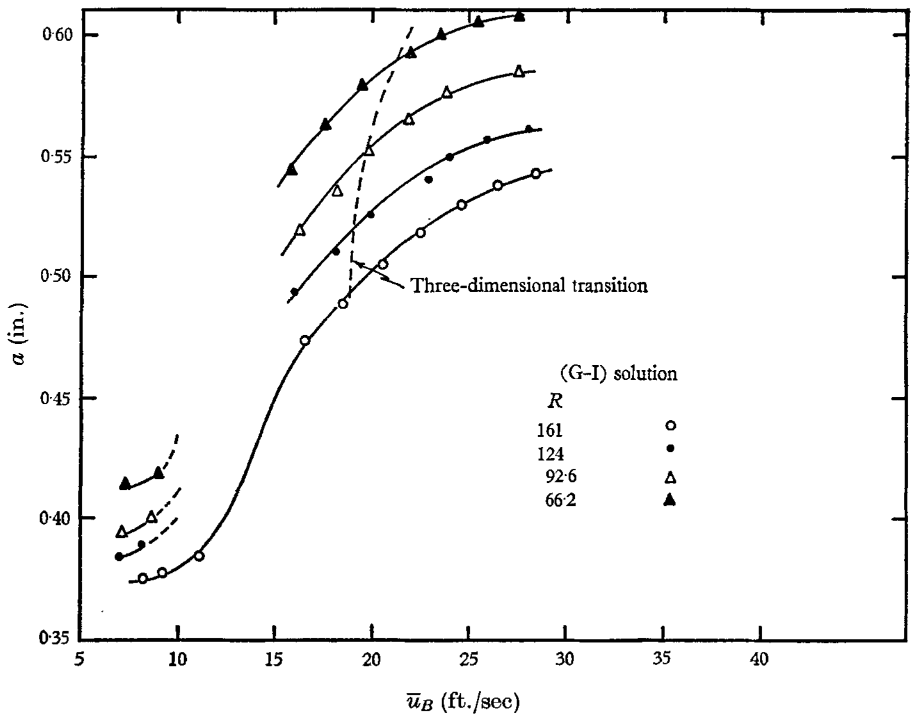

FIGURE 7. Distance from the maximum in the gas velocity profile to the interface.

Run	R	R_G	R_B	μ_L (cP)	H (in.)	a (in.)	(u_0^*ft./sec)	S
8	230	8460	9300	1·03	0·052	0·54	1·33	7·85
9	360	8440	9750	1·00	0·082	0·56	1·47	7·6

TABLE 1. Gas velocity profiles over water surface. μ_G = 0·018 cP; ρ_G = 0·072 (lb./ft.^{3}).

Two of the velocity profiles for the bottom part of the gas space are compared with velocity profiles measured in the dry channel in figure 8 and the experimental conditions are listed in table 1. The ordinate is the ratio of the velocity to the friction velocity $u^* = (\tau_0/\rho)^{\frac{1}{2}}$, designated as u^+, and the abscissa is the logarithm of the dimensionless distance from the average location of the liquid interface, y^+. The ordinate on the left side is for the runs in a dry channel. The ordinate on the right side is for the runs with liquid present. All of the data points except those representing measurements close to the centre of the channel are correlated quite well by a relation of form of (1). This is true of all of the 28 velocity profiles measured over liquid surfaces with waves. However, the slopes of these plots S, and therefore the values of K, depended on the characteristics of the interface.

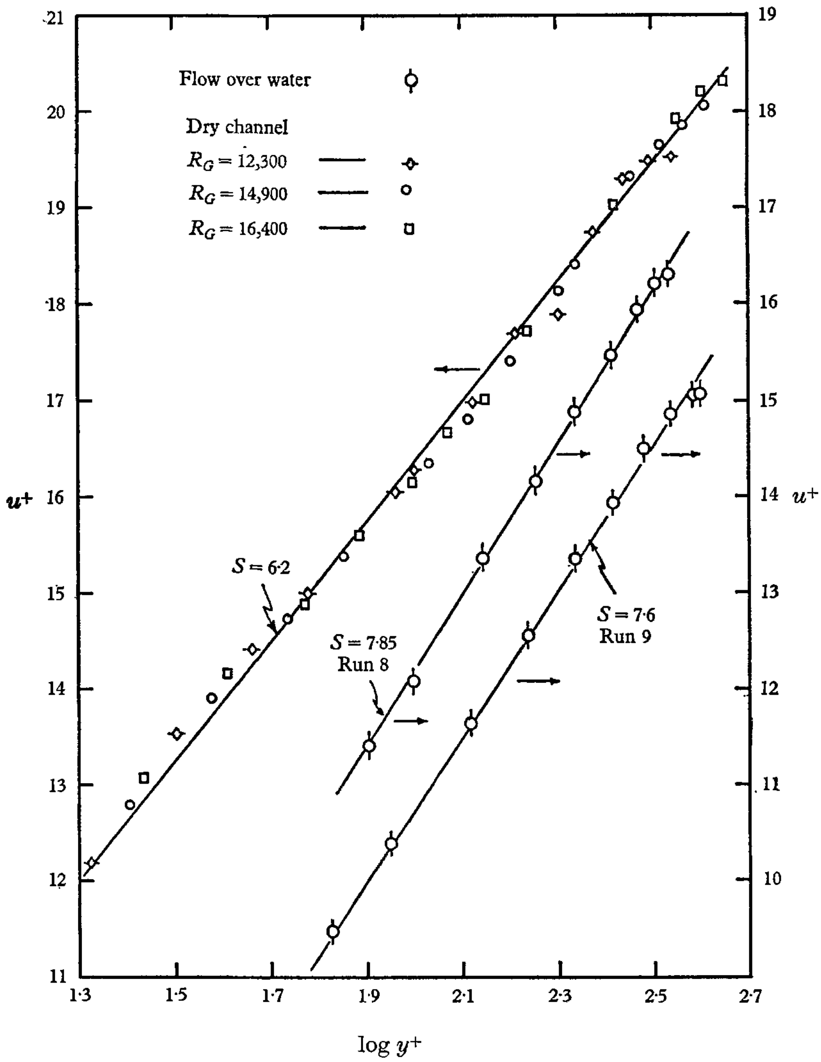

FIGURE 8. Velocity profiles.

Owing to the relatively large size of the waves it was not possible to locate the impact tube at small enough values of y to obtain very many points in the inner 20 % of the velocity profile which is usually associated with the 'law of the wall'. Therefore comparisons of the velocity data for flow over liquid surfaces to that for flow over solid surfaces had to be made on the basis of the whole velocity profile and not just the 'wall region'.

The velocity data for the dry channel shown in figure 9 correspond to Reynolds numbers which would give values of a^+ approximately equal to those for the two velocity profiles over wavy surfaces that have been plotted in the figure. The straight line through the data for the dry channel has a slope of 6·2 and therefore yields a value of K of 0·37. The lines correlating the data for flow over wavy surfaces have significantly larger slopes and yield values of K of 0·29 and 0·30. A

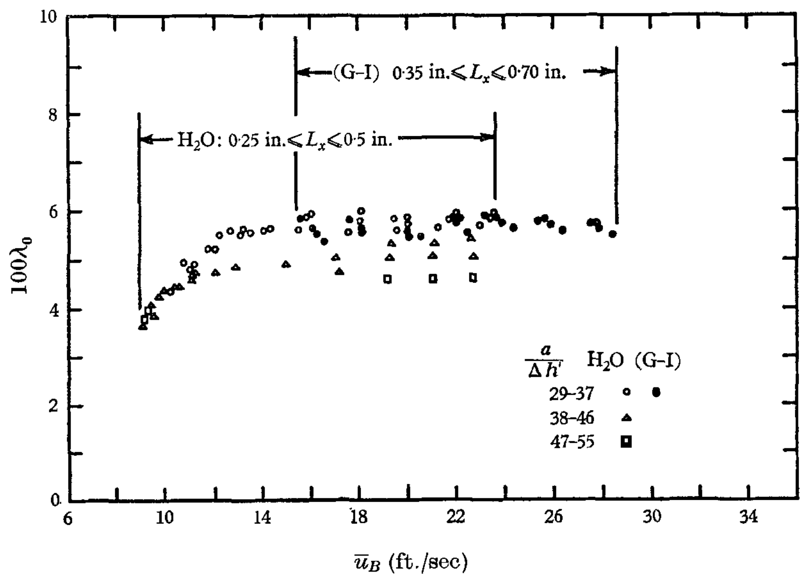

FIGURE 9. Frictional resistance at the disturbed interface.

few of the velocity profiles measured over wavy surfaces yielded values of S approximately equal to those obtained for the dry channel; however, most of them gave larger slopes.

As can be seen, parallel straight lines cannot be drawn which adequately represent the data. In this sense the velocity profiles obtained in this investigation for flow over liquid wavy surface are different from what has been reported for roughened solid surfaces. This result should not be surprising. Turbulent flow over liquid waves can be fundamentally different from that over solid waves since there is a direct exchange of mechanical energy from one phase to another in the case of liquid waves.

Consider the following approximate form of the turbulent energy equation given by Laufer (1951):

$$-\rho\,\overline{u'v'}\,\frac{du}{dy} = \frac{d}{dy}\left[\tfrac{1}{2}\rho\,\overline{v'(q^2)} + \overline{v'p'}\right] + \mu\,\overline{\left(\frac{\partial u_i'}{\partial x_j}\right)\left(\frac{\partial u_i'}{\partial x_j}\right)}, \tag{3}$$

where
$$q^2 = u'^2 + v'^2 + w'^2. \tag{4}$$

The equation states that the production of turbulent energy is balanced by the convective diffusion by turbulence of the total turbulence energy and the dissipation by the turbulent motion. If (3) is integrated over the channel cross section for flow over a solid surface the first two terms on the right side of (3) integrate out to zero. However, in flow over a wavy liquid surface $\overline{v'p'}$ is not zero at the interface and there is a net transfer of energy into the liquid. One would therefore expect that the variation of $\overline{v'p'}$ is different for flow over liquid surfaces than for flow over solid surfaces. If the transfer of energy to the liquid is appreciable one would also expect a larger production of turbulent energy in the gas for flow over liquid waves. If the velocity profile is assumed to be of the form of (1) and if

$$-\rho\,\overline{u'v'} \cong \tau_0\left(1-\frac{y}{a}\right), \tag{5}$$

then

$$-\rho\,\overline{u'v'}\frac{du}{dy} = \left(1-\frac{y}{a}\right)\frac{\rho u_0^{*3}}{Ky}. \tag{6}$$

The smaller the value of K the larger is the production of turbulent energy. This is consistent with what has been observed for the velocity profiles over liquid surfaces.

Interfacial stress

The interfacial stress measurements are correlated by defining a friction factor

$$\lambda_0 = 8(u_0^*/\overline{u}_B)^2 \tag{7}$$

in which the average velocity $\overline{u}_B$ is defined over the gas space between the interface and the maximum in the velocity profile

$$\overline{u}_B = \frac{1}{a}\int_H^{a+H} u\,dy. \tag{8}$$

The friction factors λ_0 are plotted against $\overline{u}_B$ in figure 9 with the relative roughness $a/\Delta h'$ as the parameter. In each relative roughness range at large enough $\overline{u}_B$ the friction factor assumes a constant value which is independent of both the viscosity and the characteristic, visually determined, disturbance dimension L_x. This region of constant λ_0 occurs above $\Delta h'^+ = 7$, which corresponds to the beginning of the three-dimensional wave régime. The three-dimensional waves therefore showed a behaviour similar to fully rough solid surfaces in that the interfacial stress varies as $\overline{u}_B^2$ and the friction coefficient is primarily dependent on the wave height.

An equivalent sand roughness for the liquid–air interface can be calculated by comparing the measurements of the friction factor with those of Nikuradse (Schlichting 1960). In the completely rough régime Nikuradse's results are given by

$$\frac{1}{\sqrt{\lambda_0}} = 2\log\frac{2a}{k_s} + 1{\cdot}74, \tag{9}$$

where k_s is the height of the sand roughness. Rearranging equation (9),

$$k_s^+ = \frac{k_s u^*}{\nu} = 7{\cdot}39 R_B\left(\frac{\lambda_0}{8}\right)^{\frac{1}{2}}\exp\left\{-0{\cdot}4\left(\frac{8}{\lambda_0}\right)^{\frac{1}{2}}\right\} \tag{10}$$

where $R_B = 2a\overline{u}_B/\nu$. A plot of k_s^+ against the dimensionless root-mean-square wave height $\Delta h'^+$, figure 10, shows that $k_s/\Delta h'$ increases from a value of 2 at $\Delta h'^+ = 4$ to a value of $3\sqrt{2}$ at $\Delta h'^+ = 12$. Above $\Delta h'^+ = 12$, the ratio $k_s/\Delta h'$ is essentially constant at a value of $3\sqrt{2}$.

A plot of film height versus time for three-dimensional waves is shown in figure 11. These are measurements at a fixed point in the channel. Since the wavelength is of the magnitude of 0·20 in. the surface structure at any given time would exhibit approximately the same height distribution; however, the surface slopes are much less than is indicated in the figure. The time axis should be stretched

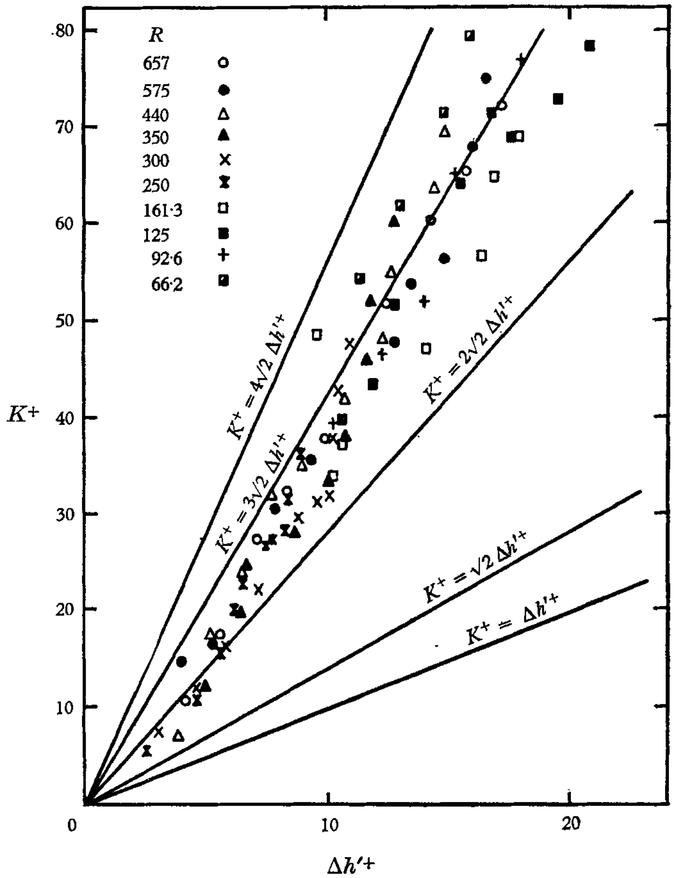

FIGURE 10. Comparison of the equivalent sand roughness with the root-mean-square wave height.

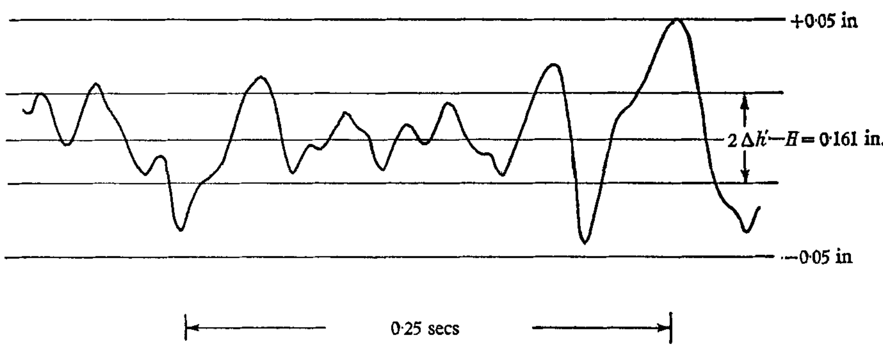

FIGURE 11. Water film height as a function of time.

out about sevenfold to give a representation of the interfacial structure. It is seen that $3\sqrt{2}\Delta h'$ corresponds approximately to the crest to peak distance of the largest waves.

Support for this research was received from the National Science Foundation under Grants G-14788, GK-62 and GK-1335.

REFERENCES

BRIGHTON, J. A. 1963 The structure of fully developed turbulent flow in annuli. Ph.D. Thesis, Purdue University.

CLAUSER, F. H. 1956 *Adv. Appl. Mech.* **4**, 1.

COHEN, L. S. 1964 Interaction between turbulent air and a flowing liquid film. Ph.D. thesis in Chemical Engineering, University of Illinois, Urbana.

DUKLER, A. 1963 *Modern Chemical Engineering*. Reinhold.

ELLIS, S. R. M. & GAY, B. 1959 *Trans. Inst. Chem. Engrs., Lond.* **37**, 206.

ELLISON, T. H. 1956 *Surveys in Mechanics*. Cambridge University Press.

HAMA, F. R. 1954 *Trans. Soc. Naval Architects Marine Engrs.* **62**, 333.

HANRATTY, T. J. & ENGEN, J. M. 1957 *A.I.Ch.E. J.* **3**, 299.

HINZE, J. O. 1961 *Colloques Internationaux du Centre National de la Recherche Scientifique, Micaneque de la Turbulence*, no. 108, Marseille.

LAUFER, J. 1951 *NACA TR*, no. 1053.

LILLELEHT, L. U. & HANRATTY, T. J. 1961*a* *J. Fluid Mech.* **11**, 65.

LILLELEHT, L. U. & HANRATTY, T. J. 1961*b* *A.I.Ch.E. J.* **7**, 548.

ROSSUM, J. J. VAN 1959 *Chem. Engng. Sci.* **11**, 35.

SCHLICHTING, H. 1960 *Boundary Layer Theory*. New York: McGraw-Hill.

URSELL, F. 1956 *Surveys in Mechanics*. Cambridge University Press.